Evaluating Four Remote Sensing Methods for Estimating Surface Air Temperature on a Regional Scale

SUHUA LIU

Key Laboratory of Water Cycle and Related Land Surface Processes, Institute of Geographic Sciences and Natural Resources Research, Chinese Academy of Sciences, and University of Chinese Academy of Sciences, Beijing, China

HONGBO SU

Department of Civil, Environmental and Geomatics Engineering, Florida Atlantic University, Boca Raton, Florida

JING TIAN AND RENHUA ZHANG

Key Laboratory of Water Cycle and Related Land Surface Processes, Institute of Geographic Sciences and Natural Resources Research, Chinese Academy of Sciences, Beijing, China

WEIZHEN WANG AND YUERU WU

Heihe Remote Sensing Experimental Research Station, Cold and Arid Regions Environmental and Engineering Research Institute, Chinese Academy of Sciences, Lanzhou, China

(Manuscript received 20 May 2016, in final form 25 October 2016)

ABSTRACT

Surface air temperature is a basic meteorological variable to monitor the environment and assess climate change. Four remote sensing methods—the temperature–vegetation index (TVX), the univariate linear regression method, the multivariate linear regression method, and the advection-energy balance for surface air temperature (ADEBAT)—have been developed to acquire surface air temperature on a regional scale. To evaluate their utilities, they were applied to estimate the surface air temperature in northwestern China and were compared with each other through regressive analyses, *t* tests, estimation errors, and analyses on estimations of different underlying surfaces. Results can be summarized into three aspects: 1) The regressive analyses and *t* tests indicate that the multivariate linear regression method and the ADEBAT provide better accuracy than the other two methods. 2) Frequency histograms on estimation errors show that the multivariate linear regression method produces the minimum error range, and the univariate linear regression method produces the maximum error range. Errors of the multivariate linear regression method exhibit a nearly normal distribution and that of the ADEBAT exhibit a bimodal distribution, whereas the other two methods display negative skewness distributions. 3) Estimates on different underlying surfaces show that the TVX and the univariate linear regression method are significantly limited in regions with sparse vegetation cover. The multivariate linear regression method has estimation errors within 1°C and without high levels of errors, and the ADEBAT also produces high estimation errors on bare ground.

1. Introduction

Near-surface air temperature T_a, which is typically measured at a height of 1.5 or 2 m at meteorological stations, is a primary variable used to assess climate change and the energy exchange between Earth's surface and the atmosphere (Prihodko and Goward 1997; Su et al. 2013). Because it plays a major role in physical processes such as photosynthesis, evapotranspiration, and heat transfer, T_a is essential in land surface process models, such as climatology, hydrology, and ecology (Lakshmi et al. 2001; Huld et al. 2006).

At present, T_a is typically monitored at meteorological stations that are deployed in a limited number of places and thus lack a broad-enough representation (Nieto et al. 2011). Hence, ground-based measurements of T_a cannot satisfy research on larger scales, such as

Corresponding author e-mail: Hongbo Su, hongbo@ieee.org; Jing Tian, tianj.04b@igsnrr.ac.cn

DOI: 10.1175/JAMC-D-16-0188.1

global climate (Prihodko and Goward 1997). The remote sensing technique is a promising alternative for obtaining spatially distributed information on the underlying surface, as it enables the assessment of environmental conditions in different ecosystems (Czajkowski et al. 1997; Goward et al. 1994). Many researchers have attempted to derive T_a through thermal infrared remote sensing data (Jang et al. 2004; Zakšek and Schroedter-Homscheidt 2009). Existing methods for acquiring T_a are mostly restricted to specific assumptions or locations, and they are divided into four groups: the temperature–vegetation index (TVX) approach (Prihodko and Goward 1997; Nieto et al. 2011; Zhu et al. 2013), the univariate linear regression method (ULRM; Chen et al. 1983; Davis and Tarpley 1983; Green and Hay 2002), the multivariate linear regression method (MLRM; Cresswell et al. 1999; Jang et al. 2004; Lin et al. 2012), and the energy balance approach (Pape and Löffler 2004; Sun et al. 2005; Hou et al. 2013).

The TVX was proposed by Nemani and Running (1989) and Goward et al. (1994) and has been successfully applied to estimate T_a by using several satellite land surface temperature (LST) products (Boegh et al. 2002; Czajkowski et al. 1997; Lakshmi et al. 2001). This method is based on the correlation between the normalized difference vegetation index (NDVI) and LST by assuming that T_a is approximately equal to the LST under a condition of full vegetation cover (Prihodko and Goward 1997; Nemani and Running 1989). If the underlying surface has partial vegetation cover, its T_a can be estimated by extrapolating full-coverage T_a values (Prince et al. 1998). The TVX has a significant advantage in that it uses NDVI and LST rather than ground-based observations as inputs. As a result, it can incorporate numerous types of data, such as Landsat ETM+ (Wloczyk et al. 2011), EOS MODIS (Yan et al. 2009), and NOAA AVHRR (Goetz 1997). Despite this unique advantage, however, the method suffers from significant uncertainties when applied to regions with sparse vegetation cover (Czajkowski et al. 1997). The linear regression methods are based on the high correlation between T_a and other variables such as LST and NDVI. The two recognized categories are the univariate linear regression method and the multivariate linear regression method. The univariate linear regression method is typically based on the linear regression between T_a and LST, whereas the multivariate linear regression method is based on the relationship between T_a and at least two other variables. There are numerous studies that have evaluated these linear regression methods. Chen et al. (1983) used LST derived from a Visible and Infrared Spin Scan Radiometer (VISSR) to simulate nighttime T_a in Florida. Subsequent validation showed a high correlation index of 0.87 and a standard deviation of 1.57 K. Davis and Tarpley (1983) used *NOAA-6* and *NOAA-7* to estimate daily minimum and maximum shelter air temperatures for monitoring agriculture, and their estimates achieved standard deviations of 1.6–2.6 K. Kawashima et al. (2000) estimated T_a on the basis of LST derived from Landsat TM; their results showed a standard error within 1.85 K. Some researchers believe that the accuracy of the multivariate linear regression method was improved by considering multiple variables that affect T_a. By using the solar zenith angle as an additional proxy for solar energy, Cresswell et al. (1999) calculated T_a from Meteosat LST data in Africa; the results showed deviations of less than 3 K for 72% of the cases. Jang et al. (2004) developed a model among five bands of the AVHRR, altitude, solar zenith angle, and yearday to derive T_a; the estimates provided a determination coefficient R^2 of 0.93 and a root-mean-square deviation (RMSD) of 1.8 K. In general, these linear regression methods perform well within the regions and time frames that they are derived from. However, they present difficulties when transferred in time and space and require a substantial dataset for training the requisite algorithms (Stisen et al. 2007).

The surface energy balance method that is used for parameterizing T_a is based on the physical mechanism that the net radiation equals the total of sensible heat flux, latent heat flux, and soil heat flux (Zakšek and Schroedter-Homscheidt 2009). Some researchers inputted net radiation, surface albedo, wind speed, and cloud cover from meteorological stations to the Meteonorm software, which was based on a simplified energy balance parameterization to calculate T_a. The results have been verified with an R^2 of 0.87 and deviations of up to 4.7 K at daytime (Meteotest 2015, p. 58). Based on variables measured by ground-based observations and derived from remote sensing, Pape and Löffler (2004) conducted research on estimating T_a in the Norwegian mountains; their results showed an R^2 of 0.9 and deviations ranging from 0.2 to 2.1 K. According to the energy balance equation, Sun et al. (2005) used aerodynamic resistance and a crop water stress index derived from MODIS data to describe the relationship between T_a and LST and then applied the relationship in northern China; the results showed deviations of less than 3 K for 80% of the cases. Hou et al. (2013) utilized Landsat TM images and applied the Bowen ratio equilibrium energy method to estimate T_a in Beijing to explore the influence of urban wetlands on the urban heat island effect; their results showed an average error of 2.21°C. The energy balance approach is a physical method that provides good portability, but it requires numeric variables that are difficult to acquire through remote sensing. In addition, the presence of advection

always characterizes exchanges near the surface layer and contributes to the uncertainty of energy influxes. In other words, advection can affect the energy balance equation and should be considered as a possible cause of imbalance when using the energy balance method to derive T_a (Spronken-Smith et al. 2000; Masson et al. 2002). Su et al. (2013) proposed an algorithm that was based on the energy balance equation and accounted for horizontal advection when retrieving T_a by remote sensing. Based on Su et al.'s research, Zhang et al. (2015) developed an advection-energy balance for surface air temperature (ADEBAT) to estimate T_a in northern China; their results were in good agreement with measurements, with an R^2 higher than 0.77 and a root-mean-square error (RMSE) lower than 0.42 K. The ADEBAT is a more reasonable version of the energy balance approach because it not only considers the local driving force regulated by the energy balance system but also accounts for the exotic driving force dominated by the advection.

Model comparison can help identify model benefits and inadequacies and can give suggestions on model development (French et al. 2015). This study evaluates four methods—the TVX, the univariate linear regression method, the multivariate linear regression method, and the ADEBAT—by applying them in northwestern China. This study primarily differs from previous studies in two aspects: 1) Although many remote sensing methods have been applied to retrieve T_a, few works have assessed them simultaneously. 2) The ADEBAT is based on the formation mechanism of air temperature, whereas the other three methods are empirical. The comparison should be significant. Section 2 introduces the four methods. Section 3 describes the study area and the dataset. Comparisons of the retrieved T_a by the four methods are presented and analyzed in section 4. Section 5 provides conclusions on the applications of the four methods, and section 6 contains the discussion.

2. Methods

To evaluate the T_a estimates retrieved by the TVX, the univariate linear regression method, the multivariate linear regression method, and the ADEBAT, it is first necessary to introduce and outline their principles.

a. The temperature–vegetation index method

The TVX is based on an empirical linear relationship between NDVI and LST. In the case of full vegetation cover, T_a is found to equal the corresponding LST (Nemani et al. 1993). The heat capacity of the surrounding air is similar to that of the dense vegetation. Hence, with the increase of vegetation cover, T_a within the canopy tends to be in equilibrium with LST of a fully vegetated canopy (Prince et al. 1998; Nieto et al. 2011).

To apply the method successfully, the TVX should assume that uniform atmospheric forcing and soil moisture conditions are in place (Stisen et al. 2007). Uniform atmospheric forcing would be satisfied on clear-sky days when the retrieval of NDVI and LST is possible, whereas uniform soil moisture is likely fulfilled by applying the TVX in a relatively small pixel array. Regression coefficients for calculating T_a are determined within a moving window around a location. Similar to most other studies concerning the TVX method, a 7×7 moving window is always applied (Zhu et al. 2013). According to our test, larger and smaller moving window sizes cannot provide enough data pairs to establish a reliable dependency between the NDVI and the LST, or they would provide overgeneralized regression parameters. On the premise of meeting the two assumptions, a linear relationship between LST and NDVI within the window can be expressed by Eq. (1):

$$\mathrm{LST} = a_i + b_i \times \mathrm{NDVI}, \tag{1}$$

where a_i and b_i are the intercept and slope of the regression line of moving window i. After establishing Eq. (1), we can derive the centered T_a of the moving window by combining the linear relation with the NDVI of dense vegetation cover. The equation used to estimate T_a can be written as

$$T_a = a_i + b_i \times \mathrm{NDVI}_{\max}, \tag{2}$$

where T_a is the estimated surface air temperature at the center of the moving window and $\mathrm{NVDI}_{\max}$ is the NDVI value of the full vegetation cover.

A critical issue of the TVX method is the definition of the $\mathrm{NVDI}_{\max}$. The air temperature can be acquired once the $\mathrm{NVDI}_{\max}$ value has been determined. According to primary studies, the $\mathrm{NVDI}_{\max}$ would vary with different study areas and different satellite images (Zhu et al. 2013; Nieto et al. 2011). In this study, we adopted the method proposed by Nieto et al. (2011) to parameterize $\mathrm{NVDI}_{\max}$, which is based on the least squares fit method using observed air temperature. The equation used to parameterize the $\mathrm{NVDI}_{\max}$ can be defined as follows:

$$T_a - a_i = b_i \times \mathrm{NDVI}_{\max}. \tag{3}$$

In Eq. (3), we know T_a, a_i and b_i; then the remaining unknown $\mathrm{NVDI}_{\max}$ can be calculated through the least squares fit method. In the study, the solving $\mathrm{NVDI}_{\max}$ was 0.76.

b. The univariate linear regression method

The heating effect of surface longwave radiation on the near-surface atmosphere accounts for the direct

energy supply of T_a; that is, the near-surface air temperature is directly driven by LST (Zhang et al. 2015; Zakšek and Schroedter-Homscheidt 2009; Stathopoulou et al. 2006). The univariate linear regression method is typically based on the strong linear regression between T_a and LST. This regression can be expressed as

$$T_a = a_0 + a_1 \times X, \tag{4}$$

where a_0 and a_1 are the regression coefficients and X is the LST (°C) or brightness temperature. According to the regression analysis, the regression equation can be written as

$$T_a = 5.9 + 0.69 \times \mathrm{LST}, \tag{5}$$

where T_a and LST are in units of degrees Celsius.

c. The multivariate linear regression method

The multivariate linear regression method accounts for not only LST but also at least two other variables that impact T_a. Land surface variables such as NDVI (Prihodko and Goward 1997), albedo (Cristóbal et al. 2008), elevation (Lin et al. 2012), and solar zenith angle (Cresswell et al. 1999) are used as proxies for reflecting T_a. In general, the multivariate linear regression method can be acquired through multiple regressions:

$$T_a = b_0 + b_1 \times X_1 + b_2 \times X_2 + \cdots + b_n \times X_n, \tag{6}$$

where b_0, b_1, b_2, . . . , b_n are regression coefficients and X_1, X_2, . . . , X_n are variables used to simulate T_a.

In this study, we first selected variables including LST, NDVI, albedo, and humidity, which are associated with surface air temperature, and then we determined coefficients of inputted variables based on stepwise linear regression. Based on the stepwise linear regression results, the selected variables and their regression coefficients are acquired [see Eq. (7)]:

$$T_a = -1.1 + 0.68 \times \mathrm{LST} + 1.67 \times \mathrm{NDVI} + 0.39 \times e_a - 2.6 \times \alpha, \tag{7}$$

where e_a (hPa) is the actual water vapor pressure, α is the albedo, and T_a and LST are also in units of degrees Celsius.

d. The ADEBAT

The ADEBAT put forward by Zhang et al. (2015) is used to derive regional T_a through remote sensing. The model assumes that the actual air temperature T_a is dominated by two physical processes: the heating effect produced by the longwave radiation from land surface (without advection, i.e., energy balance closure) and the advective effect resulting from the turbulent flow exchange. The formation of air temperature can be described as follows: the accumulation of absorbing surface longwave radiation produces a local air temperature T_{loc}, and then the advection with a temperature T_{exo} disturbs the T_{loc} by the turbulent diffusion exchange that develops between land surface and near-surface atmosphere. Hence, T_a is composed of two parts: the local air temperature T_{loc} and the exotic air temperature T_{exo}. The former can be described by the energy balance system, and the latter can be determined according to the ground-based measurements of T_a.

To calculate T_a, T_{loc} and T_{exo} should be acquired through two physical processes: the energy balance closure and the horizontal advection occurrence.

If there is no advection that means energy balance closure is satisfied, T_a is dominated by the local driving force only. The energy exchanged between the atmosphere and the underlying surface can be expressed by the energy balance equation [Eq. (8)]:

$$R_n = \mathrm{LE} + H + G, \tag{8}$$

where R_n is the net radiation, LE is the latent heat flux, H is the sensible heat flux, and G is the soil heat flux.

By combining Eq. (8) with Eq. (9) of the sensible heat flux and Eq. (10) of the Bowen ratio, T_a can be acquired:

$$H = \frac{\rho C_p}{r_a}(T_0 - T_a), \tag{9}$$

$$\beta = \frac{H}{\mathrm{LE}}, \quad \text{and} \tag{10}$$

$$T_a = \mathrm{LST} - \frac{\beta(R_n - G)}{\beta + 1}\frac{r_a}{\rho C_p}, \tag{11}$$

where ρC_p is the volumetric heat capacity of air, r_a is the aerodynamic resistance, and T_0 is the aerodynamic temperature. Since the aerodynamic temperature is difficult to determine, it is always assumed to be replaced by LST in application (Bastiaanssen et al. 1998; Su 2002). However, the assumption that LST equals the aerodynamic temperature may produce deviations in the modeled sensible heat flux, especially for semiarid and sparse vegetation areas (Kustas 1990; Lhomme et al. 2000; Norman et al. 1995; Verhoef et al. 1997; Troufleau et al. 1997). Because of the energy balance closure, T_a is equal to T_{loc}, so T_a in Eq. (11) can be replaced by T_{loc}:

$$T_{\mathrm{loc}} = \mathrm{LST} - \frac{\beta(R_n - G)}{\beta + 1}\frac{r_a}{\rho C_p}. \tag{12}$$

In Eq. (12), all necessary variables should be acquired in the case of energy balance closure. Details on these variables are available in Zhang et al. (2015).

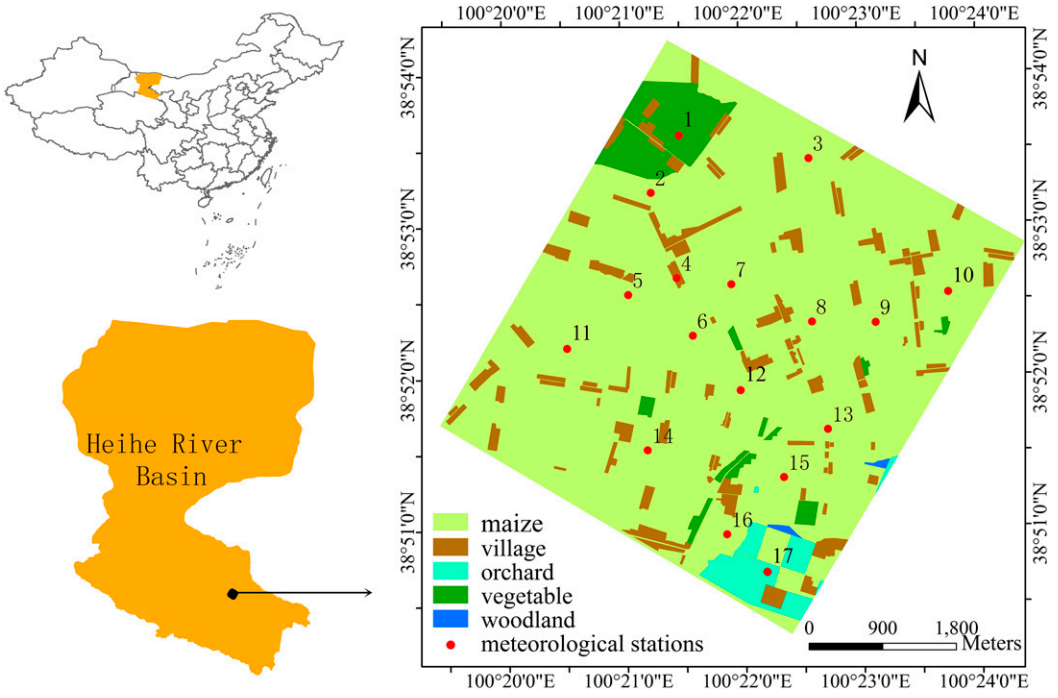

FIG. 1. Land-use status and the spatial distribution of meteorological stations in the study area.

In practice, however, the energy balance closure is not satisfied because of the exotic driving force of horizontal advection (Masson et al. 2002). In this case, the ADEBAT method uses linear mixed theory to describe T_a, which is as a mixture of T_{exo} and T_{loc} [see Eq. (13)]:

$$T_a = fT_{exo} + (1-f)T_{loc}, \tag{13}$$

$$f = \frac{V_{exo}}{V_a}, \quad \text{and} \tag{14}$$

$$1-f = \frac{V_{loc}}{V_a}, \tag{15}$$

where T_a is the real air temperature, V_a is the air volume that is equal to the sum of V_{exo} and V_{loc}, V_{exo} is the volume of the exotic air, and V_{loc} is the volume of the local air. The quantity f represents a volume percentage, which varies from 0 to 1 and also denotes the intensity of the horizontal advection on the real air temperature.

To calculate T_a in Eq. (13), two other variables, f and T_{exo}, need to be acquired with the aid of air temperature, wind speed, and wind direction measured at meteorological stations. Assuming the subscript i represents any pixel in the study area, for $f_{(i)}$ and $T_{exo(i)}$ to be calculated, the ADEBAT utilizes the wind data qualitatively to suppose that similar wind speed and direction supply similar advection and that the advection is constant within a certain area. We first selected the two nearest meteorological stations that had similar advection. If the pixels where the two meteorological stations are located are expressed as pixel 1 and pixel 2, then we can obtain the following relationships: $f_{(2)} = f_{(1)} = f_{(i)}$ and $T_{exo(2)} = T_{exo(1)} = T_{exo(i)}$. Based on Eq. (13), two new relationships can be established:

$$T_{a(1)} = f_{(1)}T_{exo(1)} + [1-f_{(1)}]T_{loc(1)} \quad \text{and} \tag{16}$$

$$T_{a(2)} = f_{(2)}T_{exo(2)} + [1-f_{(2)}]T_{loc(2)}, \tag{17}$$

where $T_{a(1)}$ and $T_{a(2)}$ are the actual air temperatures of the two meteorological stations for pixel 1 and pixel 2, and $T_{loc(1)}$ and $T_{loc(2)}$ are the local air temperatures of pixel 1 and pixel 2. By combining formulas $f_{(2)} = f_{(1)} = f_{(i)}$ and $T_{exo(2)} = T_{exo(1)} = T_{exo(i)}$ with Eqs. (16) and (17), $f_{(i)}$ and $T_{exo(i)}$ can be attained as follows:

$$f_{(i)} = 1 - \frac{T_{a(1)} - T_{a(2)}}{T_{loc(1)} - T_{loc(2)}} \quad \text{and} \tag{18}$$

$$T_{exo(i)} = \frac{[T_{a(1)} + T_{a(2)}] - [1-f_{(i)}][T_{loc(1)} + T_{loc(2)}]}{f_{(i)}}. \tag{19}$$

By combining Eq. (13) with Eqs. (18) and (19), T_a in the study area can be acquired.

In the ADEBAT, the determination of the surface roughness Z_0 in the study area is necessary because it is a key parameter used for calculating the aerodynamic resistance. In the study, we used the land-use maps (Fig. 1) to divide the study area into vegetation cover

regions (maize, orchard, vegetable, and woodland) and sparse regions (villages). In August, the vegetation is in its vigorous growth season with frequent irrigation, and the vegetation cover is dense (NDVI > 0.65). Hence, we used the empirical equation $Z_0 = 0.13h$ (h is the crop height) provided by Brutsaert (1982) to calculate the surface roughness. As for the village, we adopted research results obtained by Jia et al. (1999), who used the value of 0.04 m as surface roughness in the same study area.

3. Study area and dataset

a. Study area

The study area is located in Zhangye, China, as shown in Fig. 1 (latitude from 38.83° to 38.93°N and longitude from 100.32° to 100.42°E). The area lies in the core oasis of the middle reaches of the Heihe River, which is China's second longest inland river. The climate is dry with an annual mean air temperature of 7.0°C, an annual mean precipitation of 124.9 mm, and a potential evaporation of more than 2000 mm. The land cover in the study area consists of cropland cultivated with maize, vegetables, orchards, and woodlands. Several built-up areas (villages) are spread throughout the study area.

b. Remote sensing dataset

Remote sensing data from ASTER images and *Huan Jing* (*HJ*)-*1A*/*B* images are utilized. The ASTER sensor can collect visible, near-infrared, and thermal infrared data to monitor climate and hydrological processes (French et al. 2005). Variables such as NDVI, LST, and emissivity are derived from the ASTER images; the NDVI is easily calculated through the reflectivity of red and near-infrared bands, whereas LST and emissivity are derived from products provided by the Heihe Plan Science Data Center (Li et al. 2014). We also adopted available products provided by the Heihe Plan Science Data Center to acquire the surface albedo (Liu et al. 2014). The albedo products are calculated from images acquired from *HJ-1A*/*B*, which is a small satellite constellation used for monitoring and forecasting environmental changes and disasters. The *HJ-1A*/*B* was launched by China in 2008; two charge-coupled-device cameras are carried by each satellite, and the satellites can revisit the same place every three or four days.

c. Meteorological dataset

There are 17 automatic weather stations (AWSs) spread throughout the study area, as shown in Fig. 1. These meteorological stations measured variables including air temperature, air humidity, pressure, wind speed, land surface temperature, and solar radiation at 10-min/1-min sampling intervals (Liu et al. 2016; Xu et al. 2013). Ground-based observations are provided by Heihe Watershed Allied Telemetry Experimental Research (HiWATER)—a watershed-scale ecohydrological experiment designed from an interdisciplinary perspective to address problems such as heterogeneity, scaling, uncertainty, and closing of the water cycle at the watershed scale (Li et al. 2013). The experiment is performed in the Heihe River basin that lies in an arid region of northwestern China. Meteorological data are acquired by submitting an application to the Cold and Arid Regions Science Data Center at Lanzhou (http://westdc.westgis.ac.cn/).

TABLE 1. General descriptions of the variables and sources.

Variables	Sources
NDVI	ASTER
LST	ASTER
f_v	ASTER
ε_s	ASTER
Humidity	Meteorological stations
Wind speed	Meteorological stations
T_a	Meteorological stations
Solar radiation	Meteorological stations
Albedo	*HJ-1A*/*B*

To provide a better understanding of the data used in the study, the variables and sources applied in the study are listed in Table 1.

Two clear-sky days, 2 and 11 August 2012, are selected to retrieve T_a via the TVX, the univariate linear regression method, the multivariate linear regression method, and the ADEBAT. Because the ADEBAT requires ground-based T_a as inputs on the same day, eight meteorological stations are used as inputs; the other nine meteorological stations are used to test the results. For consistency, the other three methods also use the same nine stations and their corresponding estimations for validation purposes.

4. Results

This study conducts regressive analyses and t tests, generates frequency histograms, and compares estimates on different underlying surfaces to assess the methods. The detailed analyses from these different aspects are summarized in sections 4a–4c.

a. Regressive analyses and t tests

To test the reliability of the results acquired by the four methods, regression analyses are performed between the measurements from the meteorological stations and the respective estimates of the four methods (Fig. 2). The linear fitting equation, the R^2, the mean absolute error

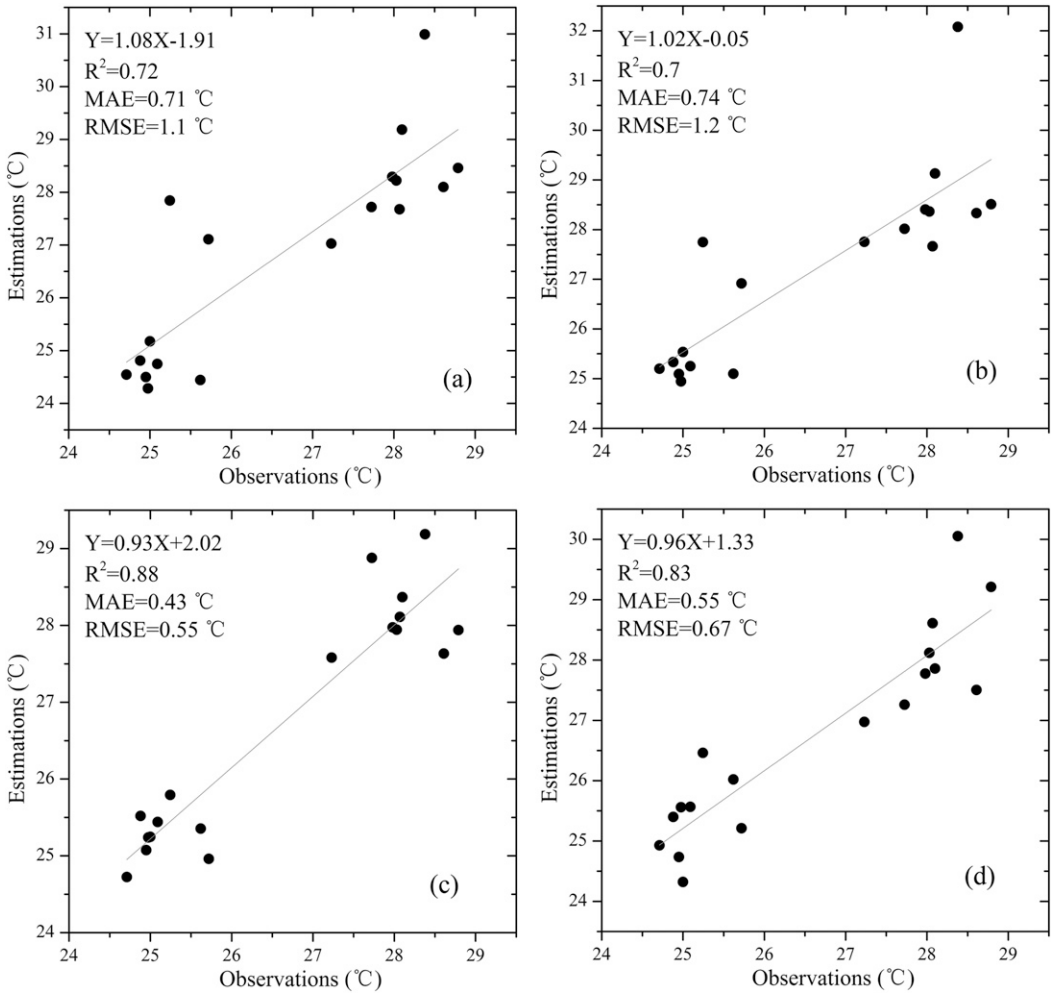

FIG. 2. Comparisons between air temperature measurements at meteorological stations and estimates from (a) the TVX, (b) the univariate linear regression method, (c) the multivariate linear regression method, and (d) the ADEBAT.

(MAE), and the RMSE are provided to describe the linear fitting results. Estimates of the TVX that were with an R^2 of 0.72, an MAE of 0.71°C, and an RMSE of 1.1°C and estimates of the univariate linear regression method that were with an R^2 of 0.7, an MAE of 0.74°C, and an RMSE of 1.2°C demonstrate lower accuracy than results obtained from the multivariate linear regression method and the ADEBAT, which have an R^2 of 0.88, an MAE of 0.43°C, and an RMSE of 0.55°C and an R^2 of 0.83, an MAE of 0.55°C, and an RMSE of 0.67°C, respectively.

It is clear that the TVX and the univariate linear regression method provide similar regression results. The multivariate linear regression method and the ADEBAT also provide similar regression results. To determine which method is more accurate and provide further distinction, paired-samples tests are performed between the MAEs of the TVX and the univariate linear regression method and between those of the multivariate linear regression method and the ADEBAT. Table 2 shows the *t*-test results between the MAEs of the TVX and the univariate linear regression method; Table 3 shows the *t*-test results between the MAEs of the multivariate linear regression method and the ADEBAT. A 5% significance level p is set as the criterion to judge if the MAE of one method is significantly different from another. The paired-samples test in Table 2 shows a p of 0.734 (significantly higher than 0.05), indicating that estimates acquired by the TVX and the univariate linear regression method exhibit no significant difference. Table 3 shows a p of 0.211 (also significantly higher than 0.05), indicating that the MAE of the multivariate linear regression method is not obviously different from that of the ADEBAT. In other words, T_a estimates from the two methods demonstrate similar accuracy.

TABLE 2. Paired-samples test between the MAEs of the TVX and the ULRM. Here, df indicates degrees of freedom.

		Paired difference							
					95% confidence interval of the difference				
		Mean	Std dev	Std error mean	Lower	Upper	t	df	Significance (two tailed)
Pair	TVX–ULRM	−0.033 43	0.410 66	0.096 79	−0.237 64	−0.170 79	−0.345	17	0.734

b. *Frequency histograms on estimation errors*

Estimation errors, that is, estimations minus corresponding in situ measurements, can provide distribution characteristics and are typically calculated when evaluating the inversion method. This study uses frequency histograms of the estimation errors to describe the error ranges. Figure 3 shows the frequency distribution of the estimation errors of the four methods. The TVX has an error range from −1.5° to ~2.5°C, with the majority of errors from −1.0° to 0.5°C, whereas the univariate linear regression method has an error range from −1.0° to ~3.5°C, with the majority of errors from −0.5° to 0.7°C. As for the other two methods, the errors of the multivariate linear regression method range from −1.0° to 1.0°C, with most of the errors between −0.5° and 0.5°C, and the ADEBAT has errors ranging from −1.2° to 1.7°C, with a large majority of errors from −0.5° to 0.5°C. The errors of the multivariate linear regression method are distributed in a nearly normal fashion and those of the ADEBAT exhibit a bimodal distribution, whereas the TVX and the univariate linear regression method have errors with negative skewness distributions. Of the four methods, the univariate linear regression method has the maximum error range, and the multivariate linear regression method has the minimum error range.

c. *Analyses of estimates on different underlying surfaces*

To explore the impact of underlying surfaces on the T_a estimates, estimations of three major land-use types (maize, villages, and orchards) on 2 and 11 August 2012 (see Tables 4 and 5, respectively) are extracted for further analyses. The TVX has estimation errors within 1.5°C on both days when the land-use types are maize and orchards, which possess dense vegetation cover. However, errors approach 2.6°C in villages that are characterized by sparse vegetation cover. This result is consistent with previous research. Jackson et al. (1981) and Williams (1994) found that the TVX produced significant estimation errors when vegetation such as individual leaves (or needles) was sparse. Czajkowski et al. (1997) also concluded that a low NDVI could significantly limit the application of the TVX and produce significant uncertainties.

The univariate linear regression method displays a situation similar to the TVX, and it had high errors of 3.1°C on average for the two days at built-up regions. The cause of this high bias is related to the density of vegetation cover. As stated in section 2, the univariate linear regression method is based on an empirical relationship between LST and T_a. The land-use map indicates that almost all meteorological stations (except the AWS 4 station) are installed in locations with dense vegetation cover. As a result, the obtained empirical equation would be more appropriate for regions with dense vegetation cover than for bare ground. In other words, the magnitude of vegetation density impacts T_a. Kawashima examined the effect of vegetation density on T_a in urban and suburban areas and determined that the influence degree of vegetation density on T_a depends on the difference between the percentages of built-up areas and vegetation areas (Kawashima et al. 2000; Kawashima 1994). Thus, we can conclude that the modeling of the univariate linear regression method is highly dependent on the location of the data capture.

As for the multivariate linear regression method, the estimated errors for the three major land-use types are all within 1°C and lack anomalies or high values. This method establishes the relationship between T_a and other

TABLE 3. Paired-samples test between the MAEs of the MLRM and the ADEBAT.

		Paired difference							
					95% confidence interval of the difference				
		Mean	Std dev	Std error mean	Lower	Upper	t	df	Significance (two tailed)
Pair	MLRM–ADEBAT	−0.114 52	0.374 05	0.088 16	−0.300 53	0.071 50	−1.299	17	0.211

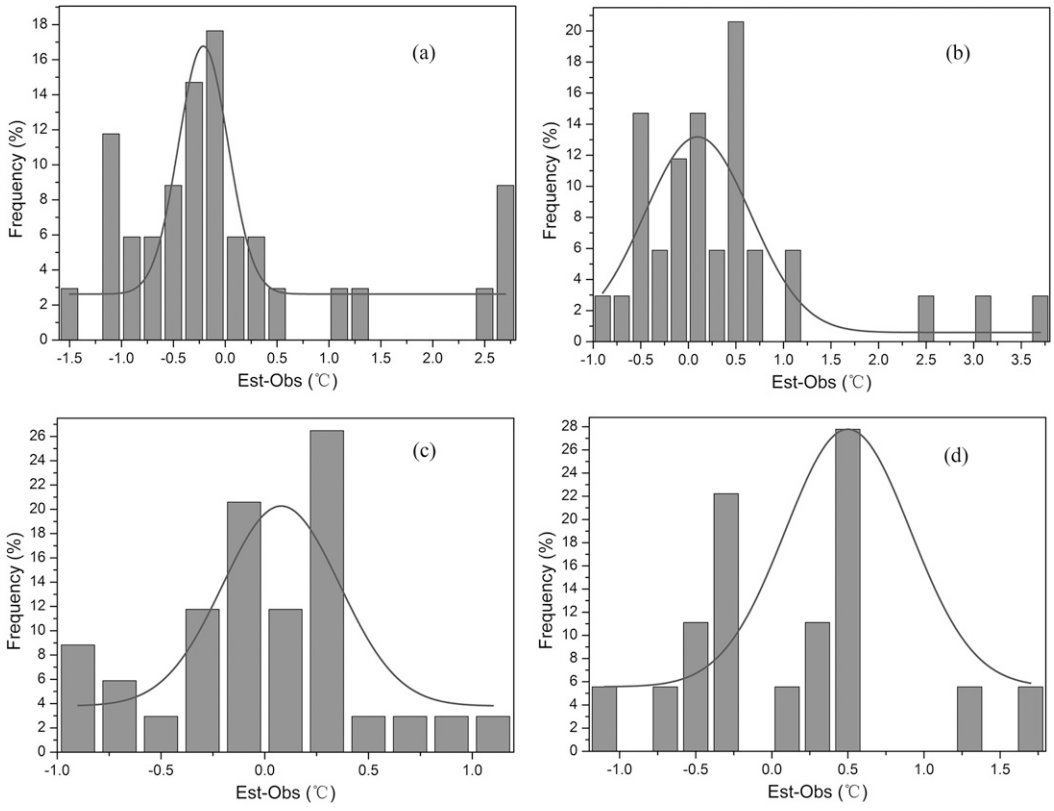

FIG. 3. Frequency histograms of estimation errors produced by (a) the TVX, (b) the univariate linear regression method, (c) the multivariate linear regression method, and (d) the ADEBAT (obs represents observations at meteorological stations; est represents estimations).

influence variables, so the calculated T_a is regulated and controlled by multiple factors such as LST, albedo, NDVI, and humidity. As a result, estimates are more accurate and less likely to generate outliers. Many previous studies have shown that the multivariate linear regression method can improve the accuracy of T_a estimates when compared with the univariate linear regression method. Kawashima et al. (2000) found that the accuracy of T_a estimates from satellite-derived surface temperature data was improved through multiple regressions by using the spatially averaged surface temperature and NDVI. Cristóbal et al. (2008) applied geographical variables such as altitude, latitude, continentality, and solar radiation along with remote sensing predictors that were most closely related to T_a such as albedo, LST, and NDVI obtained from remote sensing satellites to derive T_a by means of multiple regression analyses; they concluded that the multivariate linear regression method could decrease the RMSE.

Benefiting from the clear physical mechanism, the ADEBAT also demonstrates good accuracy on the three different underlying surfaces, with estimation errors lower than those of the TVX and univariate linear regression method. However, its estimation errors are higher than those of the multivariate linear regression method. Similar to the TVX and the univariate linear regression method, the errors of bare ground are higher than those of the other two land-use types. This may result from the assumption of the equality between LST and the aerodynamic temperature and the principle of

TABLE 4. Observations and estimations (est) of the four methods on three different underlying surfaces on 2 Aug 2012.

		TVX		ULRM		MLRM		ADEBAT	
Type	Obs	Est	Est − obs	Est	Est − obs	Est	Est − obs	Est	Est − obs
Maize	27.98	28.29	0.31	28.41	0.43	27.98	0.00	27.77	−0.21
Village	28.38	30.99	2.61	32.08	3.70	29.19	0.81	30.05	1.67
Orchard	28.10	29.19	1.09	29.13	1.03	28.37	0.27	27.86	−0.24

TABLE 5. As in Table 4, but for 11 Aug 2012.

		TVX		ULRM		MLRM		ADEBAT	
Type	Obs	Est	Est − obs	Est	Est − obs	Est	Est − obs	Est	Est − obs
Maize	25.09	24.75	−0.34	25.25	0.16	25.44	0.35	25.57	0.48
Village	25.25	27.84	2.60	27.75	2.50	25.79	0.55	26.46	1.22
Orchard	25.72	27.11	1.39	26.92	1.20	24.96	−0.76	25.21	−0.51

the ADEBAT. As for the former, the assumption that surface temperature equals the aerodynamic temperature would produce large deviations in the calculation when the underlying surfaces have sparse vegetation. As for the latter, the guiding principle of the ADEBAT requires an advection factor that should be expanded to a regional scale from a point scale. Thus, the advection factor is more appropriate in dense vegetation areas because most meteorological stations are located in places with vegetation cover.

5. Conclusions

Surface air temperature on a regional scale is significant in characterizing the energy exchange between the underlying surface and the atmosphere. The TVX, the univariate linear regression method, the multivariate linear regression method, and the ADEBAT are four major methods used for retrieving T_a through remote sensing. The former three are based on empirical correlations between T_a and other variables, whereas the ADEBAT relies on a physical formation mechanism of T_a. For the purposes of evaluation and better utilization, this study compared estimations acquired by the four methods. Results were objectively assessed by conducting regressive analyses and t tests, generating frequency histograms, and analyzing estimates on different underlying surfaces. Conclusions can be summarized as follows:

1) Through regressive analyses and t tests, we know that the multivariate linear regression method and the ADEBAT have similar accuracy, while the TVX and the univariate linear regression method have similar accuracy, and estimates of the former two methods are more accurate than those of the latter two methods.
2) Frequency histograms of estimation errors indicate that the TVX has an error range from −1.5° to ~2.5°C, whereas the univariate linear regression method has an error range from −1.0° to ~3.5°C; the error range of the multivariate linear regression method is from approximately −1.0° to ~1.0°C, whereas the ADEBAT had errors from −1.2° to 1.7°C.
3) Estimates of different underlying surfaces reveal that the TVX and the univariate linear regression method are significantly limited in regions with sparse vegetation cover. As for the other two methods, the accuracy of the multivariate linear regression method is greatly improved, with estimation errors all within 1°C for the three major land-use types; the ADEBAT has higher estimation errors on bare ground than on the other two land-use types.

6. Discussion

The TVX, the linear regression methods, and the ADEBAT are remote sensing methods for acquiring air temperature on regional scales. Each method has advantages and disadvantages. The TVX only needs LST and NDVI as inputs, and hence it can use numerous data. However, it would produce high errors in regions with sparse vegetation cover. In the study, the TVX has estimation errors up to 2.6°C for bare ground. The reason is that the TVX is an empirical method based on the relationship between LST of full coverage and NDVI, and the method would be inappropriate for sparse vegetation regions (Jackson et al. 1981; Williams 1994). The linear regression methods are based on the regression relationship between LST and other variables. The accuracy of the univariate linear regression method greatly depends on the location of data capture, and the obtained relationship would be more appropriate for similar land covers, while the accuracy of the multivariate linear regression method can be improved by multiple regressions because the method is dominated by multiple variables related to T_a, and this is in accordance with many previous studies (Kawashima et al. 2000; Cristóbal et al. 2008). About the ADEBAT, the needs of numerous variables would transfer errors and have error accumulation, and hence the estimation errors of it are higher than those of the multivariate linear regression method.

In conclusion, the TVX and linear regression methods are empirical methods based on the relationship between T_a and other variables; their principles, though lacking mechanism support for surface interactions, are easy to understand and convenient to use. However,

modeling these approaches is highly dependent on the time and location of the data capture, and an empirical equation acquired at a certain time and area would be inapplicable to other times and areas. The linear regression methods are limited by the need for a training dataset and the difficulty of spatial and temporal generalization. The ADEBAT possesses clear physical meaning and is completely different from other remote sensing methods that always neglect the formation mechanism of air temperature. Benefiting from the clear physical meaning, the ADEBAT has good portability and general applicability. However, it requires numeric variables that may be difficult to acquire through remote sensing, and estimating these variables would cause errors (Boegh et al. 2002). In addition, the ADEBAT has limitations because it depends on ground-based observations of air temperature. If a place has no adequate air temperature measurements, the ADEBAT cannot be applied successfully. The demanded amount of ground-based observations of air temperature depends on the requested accuracy, the size of the study area, and the resolution of the remote sensed images. Therefore, it is necessary to determine the data capture and accuracy demands prior to selecting a method when using these methods to estimate T_a.

Acknowledgments. This work is supported by the National Key Research and Development Program of China (Grant 2016YFA0602501), the National Natural Science Foundation of China (Grants 41571356, 41671354, and 41671373), the National Basic Research Program of China (Grant 2013CB733406), and the Key Project of National Natural Science Foundation of China (Grant 41301363). The authors declare no conflict of interest.

REFERENCES

Bastiaanssen, W. G. M., M. Menenti, R. A. Feddes, and A. A. M. Holtslag, 1998: A remote sensing surface energy balance algorithm for land (SEBAL). 1. Formulation. *J. Hydrol.*, **212–213**, 198–212, doi:10.1016/S0022-1694(98)00253-4.

Boegh, E., H. Soegaard, and A. Thomsen, 2002: Evaluating evapotranspiration rates and surface conditions using Landsat TM to estimate atmospheric resistance and surface resistance. *Remote Sens. Environ.*, **79**, 329–343, doi:10.1016/S0034-4257(01)00283-8.

Brutsaert, W. A., 1982: *Evaporation into the Atmosphere: Theory, History and Applications*. D. Reidel Publishing Company, 302 pp.

Chen, E., L. H. Allen Jr., J. F. Bartholic, and J. F. Gerber, 1983: Comparison of winter-nocturnal geostationary satellite infrared-surface temperature with shelter–height temperature in Florida. *Remote Sens. Environ.*, **13**, 313–327, doi:10.1016/0034-4257(83)90033-0.

Cresswell, M. P., A. P. Morse, M. C. Thomson, and S. J. Connor, 1999: Estimating surface air temperatures, from Meteosat land surface temperatures, using an empirical solar zenith angle model. *Int. J. Remote Sens.*, **20**, 1125–1132, doi:10.1080/014311699212885.

Cristóbal, J., M. Ninyerola, and X. Pons, 2008: Modeling air temperature through a combination of remote sensing and GIS data. *J. Geophys. Res.*, **113**, D13106, doi:10.1029/2007JD009318.

Czajkowski, K. P., T. Mulhern, S. N. Goward, J. Cihlar, R. O. Dubayah, and S. D. Prince, 1997: Biospheric environmental monitoring at BOREAS with AVHRR observations. *J. Geophys. Res.*, **102**, 29 651–29 662, doi:10.1029/97JD01327.

Davis, F. A., and J. D. Tarpley, 1983: Estimation of shelter temperatures from operational satellite sounder data. *J. Climate Appl. Meteor.*, **22**, 369–376, doi:10.1175/1520-0450(1983)022<0369:EOSTFO>2.0.CO;2.

French, A. N., and Coauthors, 2005: Surface energy fluxes with the Advanced Spaceborne Thermal Emission and Reflection Radiometer (ASTER) at the Iowa 2002 SMACEX site (USA). *Remote Sens. Environ.*, **99**, 55–65, doi:10.1016/j.rse.2005.05.015.

——, D. J. Hunsaker, and K. R. Thorp, 2015: Remote sensing of evapotranspiration over cotton using the TSEB and METRIC energy balance models. *Remote Sens. Environ.*, **158**, 281–294, doi:10.1016/j.rse.2014.11.003.

Goetz, S. J., 1997: Multi-sensor analysis of NDVI, surface temperature and biophysical variables at a mixed grassland site. *Int. J. Remote Sens.*, **18**, 71–94, doi:10.1080/014311697219286.

Goward, S. N., R. H. Waring, D. G. Dye, and J. Yang, 1994: Ecological remote sensing at OTTER: Satellite macroscale observations. *Ecol. Appl.*, **4**, 322–343, doi:10.2307/1941937.

Green, R. M., and S. I. Hay, 2002: The potential of Pathfinder AVHRR data for providing surrogate climatic variables across Africa and Europe for epidemiological applications. *Remote Sens. Environ.*, **79**, 166–175, doi:10.1016/S0034-4257(01)00270-X.

Hou, P., Y. Chen, W. Qiao, G. Cao, W. Jiang, and J. Li, 2013: Near-surface air temperature retrieval from satellite images and influence by wetlands in urban region. *Theor. Appl. Climatol.*, **111**, 109–118, doi:10.1007/S00704-012-0629-7.

Huld, T. A., M. Šúri, E. D. Dunlop, and F. Micale, 2006: Estimating average daytime and daily temperature profiles within Europe. *Environ. Modell. Software*, **21**, 1650–1661, doi:10.1016/j.envsoft.2005.07.010.

Jackson, R. D., S. B. Idso, R. J. Reginato, and P. J. Pinter Jr., 1981: Canopy temperature as a crop water stress indicator. *Water Resour. Res.*, **17**, 1133–1138, doi:10.1029/WR017i004p01133.

Jang, J.-D., A. A. Viau, and F. Anctil, 2004: Neural network estimation of air temperatures from AVHRR data. *Int. J. Remote Sens.*, **25**, 4541–4554, doi:10.1080/01431160310001657533.

Jia, L., J. Wang, and M. Menenti, 1999: Estimation of area roughness length for momentum using remote sensing data and measurements in field. *Chin. J. Atmos. Sci.*, **23**, 632–640.

Kawashima, S., 1994: Relation between vegetation, surface temperature, and surface composition in the Tokyo region during winter. *Remote Sens. Environ.*, **50**, 52–60, doi:10.1016/0034-4257(94)90094-9.

——, T. Ishida, M. Minomura, and T. Miwa, 2000: Relations between surface temperature and air temperature on a local scale during winter nights. *J. Appl. Meteor.*, **39**, 1570–1579, doi:10.1175/1520-0450(2000)039<1570:RBSTAA>2.0.CO;2.

Kustas, W. P., 1990: Estimates of evapotranspiration with a one- and two-layer model of heat transfer over partial canopy cover. *J. Appl. Meteor.*, **29**, 704–715, doi:10.1175/1520-0450(1990)029<0704:EOEWAO>2.0.CO;2.

Lakshmi, V., K. Czajkowski, R. Dubayah, and J. Susskind, 2001: Land surface air temperature mapping using TOVS and AVHRR. *Int. J. Remote Sens.*, **22**, 643–662, doi:10.1080/01431160050505900.

Lhomme, J. P., A. Chehbouni, and B. Monteny, 2000: Sensible heat flux–radiometric surface temperature relationship over sparse vegetation: Parameterizing B-1. *Bound.-Layer Meteor.*, **97**, 431–457, doi:10.1023/A:1002786402695.

Li, H., and Coauthors, 2014: Evaluation of the VIIRS and MODIS LST products in an arid area of northwest China. *Remote Sens. Environ.*, **142**, 111–121, doi:10.1016/j.rse.2013.11.014.

Li, X., and Coauthors, 2013: Heihe Watershed Allied Telemetry Experimental Research (HiWATER): Scientific objectives and experimental design. *Bull. Amer. Meteor. Soc.*, **94**, 1145–1160, doi:10.1175/BAMS-D-12-00154.1.

Lin, S., N. J. Moore, J. P. Messina, M. H. DeVisser, and J. Wu, 2012: Evaluation of estimating daily maximum and minimum air temperature with MODIS data in east Africa. *Int. J. Appl. Earth Obs. Geoinf.*, **18**, 128–140, doi:10.1016/j.jag.2012.01.004.

Liu, Q., J. Wen, S. Wu, and Y. Qu, 2014: Albedo dataset in 30m-resolution in the Heihe River Basin in 2012, Heihe Plan Science Data Center, accessed August 2014, doi:10.3972/heihe.001.2014.db.

Liu, S., and Coauthors, 2016: Upscaling evapotranspiration measurements from multi-site to the satellite pixel scale over heterogeneous land surfaces. *Agric. For. Meteor.*, **230–231**, 97–113, doi:10.1016/j.agrformet.2016.04.008.

Masson, V., C. S. B. Grimmond, and T. R. Oke, 2002: Evaluation of the Town Energy Balance (TEB) scheme with direct measurements from dry districts in two cities. *J. Appl. Meteor.*, **41**, 1011–1026, doi:10.1175/1520-0450(2002)041<1011:EOTTEB>2.0.CO;2.

Meteotest, 2015: Global meteorological database, version 7. Handbook part II: Theory. Meteonorm, Inc., 82 pp. [Available online at http://www.meteonorm.com/images/uploads/downloads/mn71_theory.pdf.]

Nemani, R. R., and S. W. Running, 1989: Estimation of regional surface resistance to evapotranspiration from NDVI and thermal-IR AVHRR data. *J. Appl. Meteor.*, **28**, 276–284, doi:10.1175/1520-0450(1989)028<0276:EORSRT>2.0.CO;2.

——, L. Pierce, S. Running, and S. Goward, 1993: Developing satellite-derived estimates of surface moisture status. *J. Appl. Meteor.*, **32**, 548–557, doi:10.1175/1520-0450(1993)032<0548:DSDEOS>2.0.CO;2.

Nieto, H., I. Sandholt, I. Aguado, E. Chuvieco, and S. Stisen, 2011: Air temperature estimation with MSG-SEVIRI data: Calibration and validation of the TVX algorithm for the Iberian Peninsula. *Remote Sens. Environ.*, **115**, 107–116, doi:10.1016/j.rse.2010.08.010.

Norman, J. M., W. P. Kustas, and K. S. Humes, 1995: Source approach for estimating soil and vegetation energy fluxes in observations of directional radiometric surface temperature. *Agric. For. Meteor.*, **77**, 263–293, doi:10.1016/0168-1923(95)02265-Y.

Pape, R., and J. Löffler, 2004: Modelling spatio-temporal near-surface temperature variation in high mountain landscapes. *Ecol. Modell.*, **178**, 483–501, doi:10.1016/j.ecolmodel.2004.02.019.

Prihodko, L., and S. N. Goward, 1997: Estimation of air temperature from remotely sensed surface observations. *Remote Sens. Environ.*, **60**, 335–346, doi:10.1016/S0034-4257(96)00216-7.

Prince, S. D., S. J. Goetz, R. O. Dubayah, K. P. Czajkowski, and M. Thawley, 1998: Inference of surface and air temperature, atmospheric precipitable water and vapor pressure deficit using Advanced Very High-Resolution Radiometer satellite observations: Comparison with field observations. *J. Hydrol.*, **212–213**, 230–249, doi:10.1016/S0022-1694(98)00210-8.

Spronken-Smith, R. A., T. R. Oke, and W. P. Lowry, 2000: Advection and the surface energy balance across an irrigated urban park. *Int. J. Climatol.*, **20**, 1033–1047, doi:10.1002/1097-0088(200007)20:9<1033::AID-JOC508>3.0.CO;2-U.

Stathopoulou, M., C. Cartalis, and N. Chrysoulakis, 2006: Using midday surface temperature to estimate cooling degree-days from NOAA-AVHRR thermal infrared data: An application for Athens, Greece. *Sol. Energy*, **80**, 414–422, doi:10.1016/j.solener.2005.02.004.

Stisen, S., I. Sandholt, A. Nørgaard, R. Fensholt, and L. Eklundh, 2007: Estimation of diurnal air temperature using MSG SEVIRI data in West Africa. *Remote Sens. Environ.*, **110**, 262–274, doi:10.1016/j.rse.2007.02.025.

Su, H., J. Tian, R. Zhang, S. Chen, Y. Yang, Y. Rong, S. Mi, and J. Qi, 2013: A physically based spatial expansion algorithm for surface air temperature and humidity. *Adv. Meteor.*, **2013**, 727546, doi:10.1155/2013/727546.

Su, Z., 2002: The Surface Energy Balance System (SEBS) for estimation of turbulent heat fluxes. *Hydrol. Earth Syst. Sci.*, **6**, 85–100, doi:10.5194/hess-6-85-2002.

Sun, Y.-J., J.-F. Wang, R.-H. Zhang, R. R. Gillies, Y. Xue, and Y.-C. Bo, 2005: Air temperature retrieval from remote sensing data based on thermodynamics. *Theor. Appl. Climatol.*, **80**, 37–48, doi:10.1007/s00704-004-0079-y.

Troufleau, D., J. P. Lhomme, B. Monteny, and A. Vidal, 1997: Sensible heat flux and radiometric surface temperature over sparse Sahelian vegetation. I. An experimental analysis of the kB^{-1} parameter. *J. Hydrol.*, **188–189**, 815–838, doi:10.1016/S0022-1694(96)03172-1.

Verhoef, A., H. A. R. De Bruin, and B. J. J. M. Van Den Hurk, 1997: Some practical notes on the parameter kB^{-1} for sparse vegetation. *J. Appl. Meteor.*, **36**, 560–572, doi:10.1175/1520-0450(1997)036<0560:SPNOTP>2.0.CO;2.

Williams, D. L., 1994: The radiative transfer characteristics of spruce (Picea spp.): Implications relative to the canopy microclimate. Ph.D. dissertation, University of Maryland, College Park, 113 pp.

Wloczyk, C., E. Borg, R. Richter, and K. Miegel, 2011: Estimation of instantaneous air temperature above vegetation and soil surfaces from *Landsat 7* ETM+ data in northern Germany. *Int. J. Remote Sens.*, **32**, 9119–9136, doi:10.1080/01431161.2010.550332.

Xu, Z., and Coauthors, 2013: Intercomparison of surface energy flux measurement systems used during the HiWATER-MUSOEXE. *J. Geophys. Res. Atmos.*, **118**, 13 140–13 157, doi:10.1002/2013JD020260.

Yan, H., J. Zhang, Y. Hou, and Y. He, 2009: Estimation of air temperature from MODIS data in east China. *Int. J. Remote Sens.*, **30**, 6261–6275, doi:10.1080/01431160902842375.

Zakšek, K., and M. Schroedter-Homscheidt, 2009: Parameterization of air temperature in high temporal and spatial resolution from a combination of the SEVIRI and MODIS instruments. *ISPRS J. Photogramm. Remote Sens.*, **64**, 414–421, doi:10.1016/j.isprsjprs.2009.02.006.

Zhang, R., Y. Rong, J. Tian, H. Su, Z.-L. Li, and S. Liu, 2015: A remote sensing method for estimating surface air temperature and surface vapor pressure on a regional scale. *Remote Sens.*, **7**, 6005–6025, doi:10.3390/rs70506005.

Zhu, W., A. Lu, and S. Jia, 2013: Estimation of daily maximum and minimum air temperature using MODIS land surface temperature products. *Remote Sens. Environ.*, **130**, 62–73, doi:10.1016/j.rse.2012.10.034.